J. of Supercritical Fluids 59 (2011) 157–167

Contents lists available at ScienceDirect

The Journal of Supercritical Fluids

journal homepage: www.elsevier.com/locate/supflu

Fabrication of porous PCL/elastin composite scaffolds for tissue engineering applications

Nasim Annabi[a], Ali Fathi[a], Suzanne M. Mithieux[b], Anthony S. Weiss[b], Fariba Dehghani[a,*]

[a] School of Chemical and Biomolecular Engineering, University of Sydney, Sydney 2006, Australia
[b] School of Molecular Bioscience, University of Sydney, Sydney 2006, Australia

ARTICLE INFO

Article history:
Received 10 February 2011
Received in revised form 17 June 2011
Accepted 19 June 2011

Keywords:
Gas foaming-salt leaching
Composite scaffold
Elastin
PCL
Porosity

ABSTRACT

We present the development of a technique that enables the fabrication of three-dimensional (3D) porous poly(ε-caprolactone) (PCL)/elastin composites. High pressure CO_2 was used as a foaming agent to create large pores in a PCL matrix and impregnate elastin into the 3D structure of the scaffold. The effects of process variables such as temperature, pressure, processing time, depressurization rate, and salt concentration on the characteristics of PCL scaffolds were determined. Scaffolds with average pore sizes of 540 μm and porosity of 91% were produced using CO_2 at 65 bar, 70 °C, processing time of 1 h, depressurization rate of 15 bar/min, and addition of 30 wt% salt particles. The PCL/elastin composites were then prepared under different conditions: ambient pressure, vacuum, and high pressure CO_2. The fabrication of composites under vacuum resulted in the formation of nonhomogenous scaffolds. However, uniform 3D composites were formed when using high pressure CO_2 at 37 °C and 60 bar.

1. Introduction

Polymers are used for the fabrication of hydrogel scaffolds in tissue engineering. These polymeric scaffolds are intended to support biological function by promoting the adhesion, differentiation, and viability of cells [1] and also to provide sufficient mechanical strength for the formation of functional engineered tissue [2]. Extracellular matrix (ECM) proteins such as collagen and elastin interact with cells via cell surface receptors and regulate or direct cell function [3]. However, their utility as hydrogel scaffolds has been limited by their poor mechanical properties. Synthetic biodegradable polymers such as poly(ε-caprolactone) (PCL), unlike natural ECM components, do not have specific cell-binding sites but do have superior mechanical strength [4,5]. The fabrication of hybrid synthetic/natural scaffolds allows for the incorporation of a suitable balance of biological and mechanical properties.

1.1. Fabrication of composite scaffolds

Various methods have been used to combine natural and synthetic polymers for tissue engineering applications. Hybrid PCL/collagen films were fabricated by impregnation of freeze-dried collagen films with a solution of PCL in dichloromethane followed by evaporation of solvent [6]. The fabricated composite scaffolds had pore sizes ranging from 50 to 100 μm and could support the growth of human osteoblasts [6]. Two-dimentional (2D) PCL/natural polymer composite films have been prepared by coating PCL films prepared by solvent casting with biomimetic ECM components such as fibrin, gelatin, and fibronectin [7]. The fabricated composites significantly promoted endothelial cells adhesion and proliferation compared to pure PCL film [7]. Chen et al. fabricated collagen/poly(D,L-lactide-co-glycolide) (PLGA) scaffolds by embedding collagen fibers within a PLGA matrix [8]. In this method, PLGA sponges were prepared by a solvent casting/particle leaching technique using NaCl particles as the porogen and chloroform as the solvent [8]. The sponges were then immersed in an acidic collagen solution under vacuum to fill the pores of PLGA with collagen [8]. The composites were freeze-dried and subsequently cross-linked with glutaraldehyde (GA) vapor [8]. The Young's Modulus of the fabricated composite was 1.23 MPa which was higher than that of either PLGA (0.7 MPa) or collagen (0.2 MPa) [8]. A problem with the use of organic solvent in these methods is that any residue left in the material may be cytotoxic [9]. Electrospinning using natural and synthetic polymers can give hybrid natural/synthetic scaffolds [10,11]. Electrospinning was used to fabricate hybrid scaffolds comprised of PCL and natural proteins such as collagen, elastin, and gelatin, by dissolving them in hexafluoro-2-propanol [12]. The addition of PCL had no significant impact on porosity, but increased the mechanical properties of composites compared to protein alone. Collagen/elastin/PCL scaffolds presented pore sizes ranging from 8 to 39 μm and Young's Modulus between 25 MPa and 35 MPa

* Corresponding author. Tel.: +61 2 93514794; fax: +61 2 93512854.
E-mail address: fariba.dehghani@sydney.edu.au (F. Dehghani).

0896-8446/$ – see front matter.
doi:10.1016/j.supflu.2011.06.010

[12]. Elastin can also be combined with other synthetic polymers such as PLGA to produce hybrid electrospun biomaterials with improved mechanical properties for vascular applications where the modulus must be greater than 500 kPa [11]. The low thickness of fabricated scaffolds and residual organic solvent (e.g. hexafluoro-2-propanol) are major issues involved with using electrospinning for the formation of natural/synthetic composite scaffolds.

1.2. Fabrication of porosity

Cell adhesion and proliferation in scaffolds can be promoted by generating porosity within the 3D constructs [13]. Porosity is induced in polymeric matrices using a variety of methods including electrospinning, freeze-drying, and solvent casting/salt leaching [2]. However, the disadvantages of these techniques include the use of toxic organic solvent, formation of thin 2D structures, non-homogenous and limited porosity, irregularly shaped pores, and insufficient pore interconnectivity [2].

Gas foaming process using high pressure CO_2 has been widely employed to eliminate the problems associated with the use of these conventional methods for porosity generation. Porous structures of amorphous or semi-crystalline hydrophobic polymers such as poly(lactic) acid (PLA), PLGA, PCL, poly(methyl methacrylate) (PMMA) and polystyrene have been obtained using gas foaming technique [14–17]. There are three basic steps in this process: (a) polymer plasticization due to CO_2 diffusion into the polymer matrix with increasing pressure, (b) nucleation of gas bubbles as a result of depressurization and supersaturation, and (c) nucleation growth due to the gas diffusion from the surrounding polymer [16,18]. The formation of a non-porous external skin layer [19,20] and lack of interconnectivity between pores [21] due to the rheological and processing limitations are common issues in gas foaming technique. Gas foaming/salt leaching methods have been developed to address these issues [22,23]; for example Salerno et al. produced PCL foams with porosity in the range of 78–93% and pore sizes between 10 and 90 μm [23]. However, the gas foaming technique is not efficient for the creation of porosity in crystalline and hydrophilic polymers.

Recently we developed a technique to create porosity in composite tropoelastin/elastin hydrogels using high pressure CO_2 [24]. These composite hydrogels are formed in an aqueous phase without using any surfactant. The compressive modulus of the fabricated composite hydrogels increases 2-fold from 6.1 kPa to 11.8 kPa when high pressure CO_2 is used compared to hydrogels produced at 1 bar [24]. Further enhancement in mechanical properties of fabricated elastin-based hydrogels is required for engineering of load bearing tissues.

The aim of this study was to develop a rapid and solvent free process for the fabrication of homogenous PCL/elastin hybrid scaffolds suitable for tissue engineering applications, particularly bone and cartilage repair. Elastin is an insoluble ECM protein that provides various tissues in the body with the properties of extensibility and elastic recoil [25]. PCL is a biodegradable and biocompatible polyester with a low glass transition temperature (−60 °C) and melting point (60 °C), which make it easy to process [7]. PCL membranes elongate up to 1000% before break, which displays its high mechanical strength [4,5]. The results of our previous *in vitro* studies demonstrate that the addition of elastin to PCL dramatically promotes chondrocyte adhesion to PCL scaffolds [26]. In this study, the feasibility of using gas foaming/salt leaching technique for the creation of large pores (i.e. >500 μm) in PCL was assessed. The efficiency of high pressure CO_2 and vacuum for impregnation of elastin into the PCL porous structure to fabricate PCL/elastin composites was assessed by SEM, FTIR, weight gain elastin stability, and swelling ratio measurements.

2. Materials and methods

2.1. Materials

α-Elastin extracted from bovine ligament was purchased from Elastin Products Co. (MO, USA). PCL (M_W = 80 kDa, T_m = 60 °C, T_g = −60 °C), GA and NaCl were purchased from Sigma–Aldrich. Food grade carbon dioxide (99.99% purity) was supplied by BOC. NaCl particles were ground and sieved to generate particles in the range of 100–700 μm.

2.2. Fabrication of PCL/elastin composite scaffolds

The schematic diagram for producing composite PCL/elastin scaffolds is illustrated in Fig. 1. The fabrication of hybrid scaffolds is characterized by four steps: (1) preparation of the PCL/NaCl blend by melt mixing; (2) gas foaming of the PCL/NaCl composite using dense gas CO_2; (3) leaching out the salt particles from the PCL scaffold; (4) embedding elastin into the PCL scaffold and cross-linking under either high pressure CO_2, atmospheric conditions or vacuum.

2.3. Formation of porous PCL scaffold

Experiments were conducted to determine the effects of gas foaming processing parameters on the pore characteristics of PCL. Process variables include saturation temperature (T_s), saturation pressure (P_s), soaking time (S_t), depressurization rate (DPR), salt particle size and concentration. In each run, PCL was first melted at 60 °C and blended for at least 10 min with NaCl particles. The blend was then placed in a custom-made Teflon mold and cooled at 25 °C for 10 min to form disk-shaped samples (d = 5 mm, h = 3 mm).

A gas foaming process was then used to fabricate porous PCL scaffolds. The same experimental set-up as in our previous study was used for the gas foaming process [24]. In each run, a PCL/NaCl disk was placed inside a high pressure vessel (Thar, 100 ml view cell). The system was then pressurized with CO_2 to a predetermined P_s using a syringe pump (ISCO, Model 500D) and the pump was then run at constant pressure mode. The temperature was increased to the desired T_s using the Thar reactor temperature controller; the system was maintained at these conditions for a set period of S_t. The temperature was then gradually decreased to a foaming temperature of 34 °C at which point the inlet valve was closed and the system was depressurized at a predetermined DPR.

Fabricated PCL/NaCl samples were soaked in MilliQ water at room temperature for 24 h to leach out salt particles and then dried. Salt leaching ratio (φ) measurements were used to determine the amount of NaCl leached out from the PCL scaffolds using the following equation:

$$\varphi = \frac{(W_b - W_a)/W_b}{C_{NaCl}} \times 100$$

where W_b is the weight of the PCL/NaCl sample before salt leaching, W_a is the weight of the PCL scaffold, and C_{NaCl} is the initial concentration of NaCl in PCL/NaCl blend.

2.3.1. Fabrication of composite PCL/elastin scaffolds

Porous PCL scaffolds were soaked in an aqueous solution containing 5% (w/v) elastin and 0.25% (v/v) GA at 37 °C to fabricate composite scaffolds. Three different operating conditions comprising atmospheric pressure, vacuum, and high pressure CO_2 were used for embedding and cross-linking of elastin into the 3D structure of PCL. The cross-linking reaction was conducted for a period of 24 h when atmospheric pressure and vacuum (−1 MPa) were used to form the composites. The fabricated constructs were then washed repeatedly in PBS (10 mM phosphate, 150 mM NaCl; pH 7.4), and then placed in 100 mM Tris in PBS for 1 h to quench the

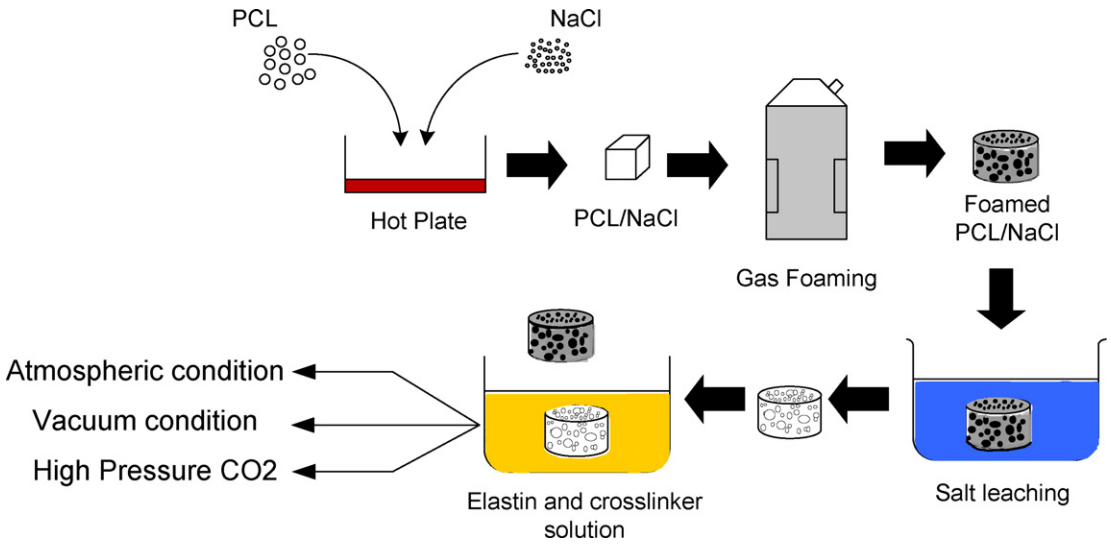

Fig. 1. Schematic diagram for the production of PCL/elastin composite scaffolds.

cross-linking reaction. After Tris treatment, the composite scaffolds were washed twice and stored in PBS.

The gas foaming apparatus was used for the preparation of PCL/elastin hybrid scaffolds at high pressure. The PCL scaffold was placed in a Teflon mold inside a high pressure vessel; elastin solution containing GA was then injected into the mold. After the vessel was sealed and equilibrated at 37 °C, the system was pressurized with CO_2 to 60 bar, isolated and maintained under these conditions for 1 h. The system was then depressurized at 15 bar/min and the sample was collected. The fabricated composite scaffold then quenched with Tris as described above.

Gravimetric analysis was used to determine the amount of elastin embedded in the 3D PCL scaffolds using the following equation:

$$\text{Weight gain} = \frac{W_{\text{Composite}} - W_{\text{PCL}}}{W_{\text{PCL}}} \times 100$$

where $W_{\text{composite}}$ is the weight of the PCL/elastin composite scaffold and W_{PCL} is the weight of PCL scaffold.

2.3.2. Scanning electron microscopy (SEM)

SEM images of samples were obtained using a Zeiss Qemscan at 15 kV to determine the pore characteristics of the fabricated PCL scaffolds and to examine the penetration of elastin into the 3D structures of PCL matrices. Lyophilized constructs were mounted on aluminum stubs using conductive carbon paint then gold coated prior to SEM analysis.

2.4. Average pore size and porosity calculation

Image J software was used to calculate the equivalent circle diameter (ECD) of the pores using SEM images. For each sample several SEM images were taken. The sizes of at least 100 pores were measured using the Image J Software and the average pore sizes was then calculated.

Porosity of the scaffolds was calculated using the following equation:

$$\text{Porosity} = \frac{A_{\text{p}}}{A_{\text{T}}}$$

where A_{p} is total area of pores in each cross section and A_{T} is the total area of each cross section. Image J Software was used to calculate A_{p} and A_{T}. For each sample at least ten SEM images were analyzed and the average porosity for each group of images was measured.

2.5. Fourier transform infrared (FTIR) spectrometer

FTIR analysis was used to qualitatively characterize the functional groups of elastin and PCL, and to confirm the 3D penetration of elastin into the PCL scaffolds. FTIR spectra were collected at the resolution of 2 cm^{-1} and signal average of 32 scans in each interferogram over the range of 1900–1400 cm^{-1} using a Varian 660 IR FTIR spectrometer. Composite scaffolds with thickness of 3 mm were used for FTIR analysis. The depth of elastin penetration into the PCL scaffolds was evaluated by performing FTIR analysis on the top surface and two layers manually cut from within the composites (i.e. 1 mm and 2 mm below the surface).

2.6. Water uptake properties

The water uptake ratios of PCL scaffold and PCL/elastin composites produced under high pressure CO_2 and vacuum were measured at 37 °C in PBS solution. The scaffolds were lyophilized to calculate their dried weight. The samples were then soaked in 10 ml PBS for 24 h. The excess liquid was removed from the samples and the water uptake was calculated based on a ratio of the increase in mass to that of the dry sample. The reported data at each condition was the average measurement for at least three scaffolds.

2.7. Elastin retention/stability ratio measurement

The stability of embedded crosslinked elastin within the 3D structures of composites was evaluated by immersing PCL/elastin composites fabricated under high pressure CO_2 in PBS solution at 37 °C for up to 7 days. The composites were taken out of the PBS solution at time intervals of 1, 2 and 7 days, washed with distilled water, freeze-dried and weighed. Elastin retention ratio measurement was used to determine the amount of elastin remaining within the 3D structures of composite scaffolds after soaking in PBS solution at different time intervals, using the following equation:

$$\text{Elastin retention ratio} = \frac{(W_{\text{composite}} - W_{\text{PCL}})_{\text{b}}}{(W_{\text{composite}} - W_{\text{PCL}})_{\text{a}}} \times 100$$

$(W_{composite} - W_{PCL})_a$ and $(W_{composite} - W_{PCL})_b$ represent the weight of the elastin within the PCL scaffold after and before immersion in PBS solution for a given time, respectively.

2.8. Statistical analysis

Data is reported as mean ± STD. One-way analysis of variance (ANOVA) with Bonferroni post hoc tests for multiple comparisons was performed using SPSS software for Windows version 18.0.1. Statistical significance was accepted at $p < 0.05$ and indicated in the figures as $^{*}p < 0.05$, $^{**}p < 0.01$, and $^{***}p < 0.001$.

3. Results and discussion

The objective of this study was to create PCL/elastin composites with a large average pore size and a high degree of pore interconnectivity that could potentially be used for load-bearing tissue engineering applications including cartilage replacement. Chrondrocyte proliferation and ECM production in gelatin scaffolds can be seen when the pore sizes are in the range of 250–500 μm [13]. On this basis, PCL scaffolds were fabricated with pore sizes larger than 500 μm so that following the subsequent elastin impregnation process, the PCL/elastin composites would retain pore sizes suitable for cellular penetration and growth.

Preliminary results for gas foaming neat PCL demonstrated that the process was not efficient for creating large interconnected pores. A skin layer was formed on the top surface of scaffold, when the gas foaming process was conducted at 65 bar, 70 °C for 1 h, and DPR of 15 bar/min; at these conditions the pore size was less than 150 μm throughout the cross-section of sample. This result was in agreement with previous studies where PCL scaffolds with average pore sizes of 150 μm were obtained at 250 bar, 40 °C, and DPR of 20 bar/min [27]. It has been demonstrated that the addition of NaCl particles to polymer as a hardening agent can increase pore-wall opening during foaming and enhance pore interconnectivity [23]. A gas foaming/salt leaching process was therefore investigated as a means of fabricating large interconnected pores in PCL scaffolds. Gas foaming process parameters, NaCl particle size and concentration were manipulated to tailor the pore characteristics of PCL scaffolds.

3.1. Effect of salt

The effects of NaCl particle size (i.e. 100–300 μm, 300–500 μm, and 500–700 μm) and concentrations (30 wt%, 60 wt%) on pore characteristics and the leaching ratio (φ) were determined. For this investigation, gas foaming process was conducted at 65 bar, 70 °C, using S_t of 1 h and DPR of 15 bar/min. A salt concentration of 30 wt% was used to determine the effect of NaCl particle sizes on pore morphology of fabricated PCL scaffolds. There was a correlation between the pore size of fabricated scaffold and salt particle size; as shown in Figs. 2 and 3A, increasing the salt particles from 100–300 μm to 300–500 μm significantly enhanced the pore sizes of PCL scaffolds from 175 ± 20 μm to 390 ± 15 μm ($p < 0.01$). The highest average pore size of 540 ± 18 μm and porosity of 91.1 ± 1.2% were obtained when porogen particle sizes of 500–700 μm were used Fig. 3. The normalized PCL pore size distributions using various ranges of salt particle sizes are shown in Fig. 4. As shown in Fig. 4A, using a particle size range of 100–300 μm resulted in generating pores with average size less than 400 μm. The percentage of pores larger than 400 μm approached 45% and 70% by increasing the porogen particle size to 300–500 μm and 500–700 μm, respectively (Fig. 4B and C).

Salt particle sizes in the range of 500–700 μm were used to determine the effect of NaCl concentrations. As indicated in Figs. 2 and 3A, the pore sizes of PCL scaffolds significantly increased from 310 ± 15 μm to 540 ± 18 μm by decreasing the NaCl concentration from 60 wt% to 30 wt%, respectively ($p < 0.001$). Increasing salt concentration from 30 wt% to 60 wt% significantly decreased the porosity of the fabricated scaffold from 91.1 ± 1.2% to 50 ± 1.2% ($p < 0.001$), as shown in Fig. 3B. In addition, φ was enhanced from 70% to 100%, when the salt concentration was reduced from 60 wt% to 30 wt%. Salerno et al. observed a similar behavior for the effect of salt concentration on pore characteristics; PCL scaffolds with

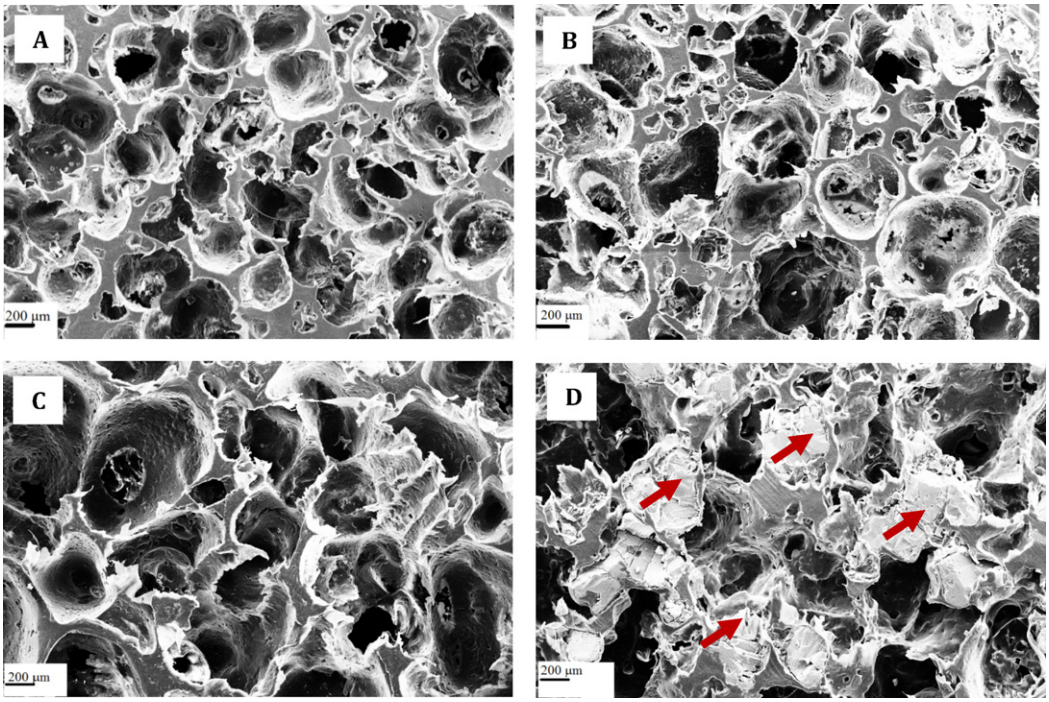

Fig. 2. SEM images of PCL scaffolds fabricated by the gas foaming/salt leaching process, using salt particle sizes of 100–500 μm (A), 300–500 μm (B), and 500–700 μm (C and D). (Salt concentrations of 30 wt% were used in (A–C), and 60 wt% in (D); arrows show salt particles within pores of PCL scaffold.)

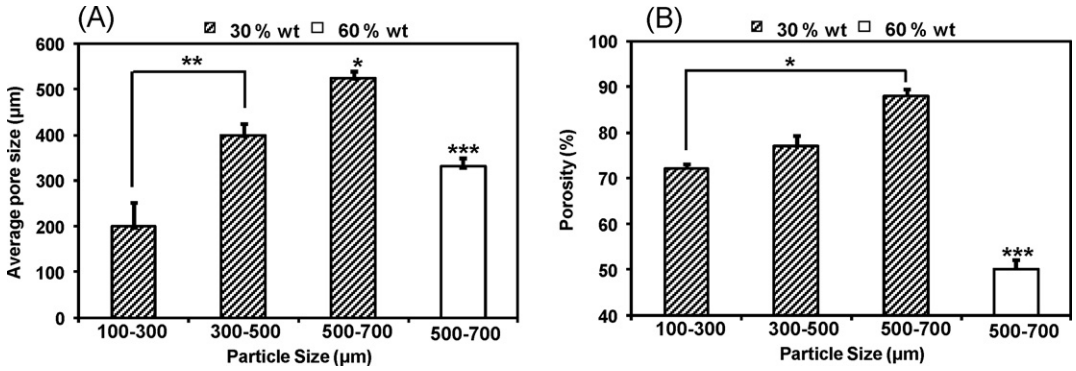

Fig. 3. Effect of salt particle size and concentration on the pore sizes (A) and porosity (B) of PCL scaffolds fabricated by the gas foaming/salt leaching process.

average pore size of 100 μm and 87% pore interconnectivity were produced using CO_2 at 65 bar, 70 °C for 3 h, and 30 wt% salt concentration [23]. These pore characteristics are not suitable for cartilage tissue engineering where pore sizes in the range of 250–500 μm are required [13].

Reduction in the pore sizes of fabricated scaffold, using 60 wt% NaCl, might be due to an increase in the stiffness of the PCL/NaCl blend, which resulted in limited CO_2 diffusion. Consequently, the porosity of scaffolds was decreased from 91.1 ± 1.2% to 50 ± 1.2%, by increasing the NaCl concentration from 30 wt% to 60 wt%. Salt particles were entrapped inside the structure of PCL scaffolds fabricated using 60 wt% NaCl, as shown in Fig. 2D. At this salt concentration, pores were mainly formed by gas foaming (<150 μm) and less pores were formed by salt leaching. Therefore, the average pore size of scaffold fabricated with 60 wt% NaCl was 320 μm, which was lower than the size of salt particle (500–700 μm) that were used.

It is critical to create highly interconnected pores with average size above 500 μm in PCL scaffold to facilitate both elastin penetration and cell proliferation in 3D structure. The presence of pore interconnectivity and large pore sizes can minimize surface tension and facilitate elastin penetration into the porous structure of PCL. In this study, porogen concentration of 30 wt% and particle size in the range of 500–700 μm were used to fabricate PCL scaffolds.

3.2. Effect of gas foaming

Manipulation of processing parameters including P_s, T_s, DPR, and S_t during gas foaming allow for control over the porous architecture of fabricated PCL scaffolds (Table 1). Preliminary results demonstrated that a non-uniform porous PCL scaffold was produced when the depressurization stage was conducted at temperatures above 34 °C. Di Maio et al. also reported that using foaming temperatures above 34 °C resulted in the formation of non-homogeneous PCL structures consisting of few large pores [28]. The formation of non-uniform pores in PCL structures can be due to PCL melting at high pressures and its inability to crystallize. Coalescence phenomena are likely to occur because of the low viscosity of PCL, which would not permit a complete stabilisation of the cellular structure. Therefore, in this study a foaming

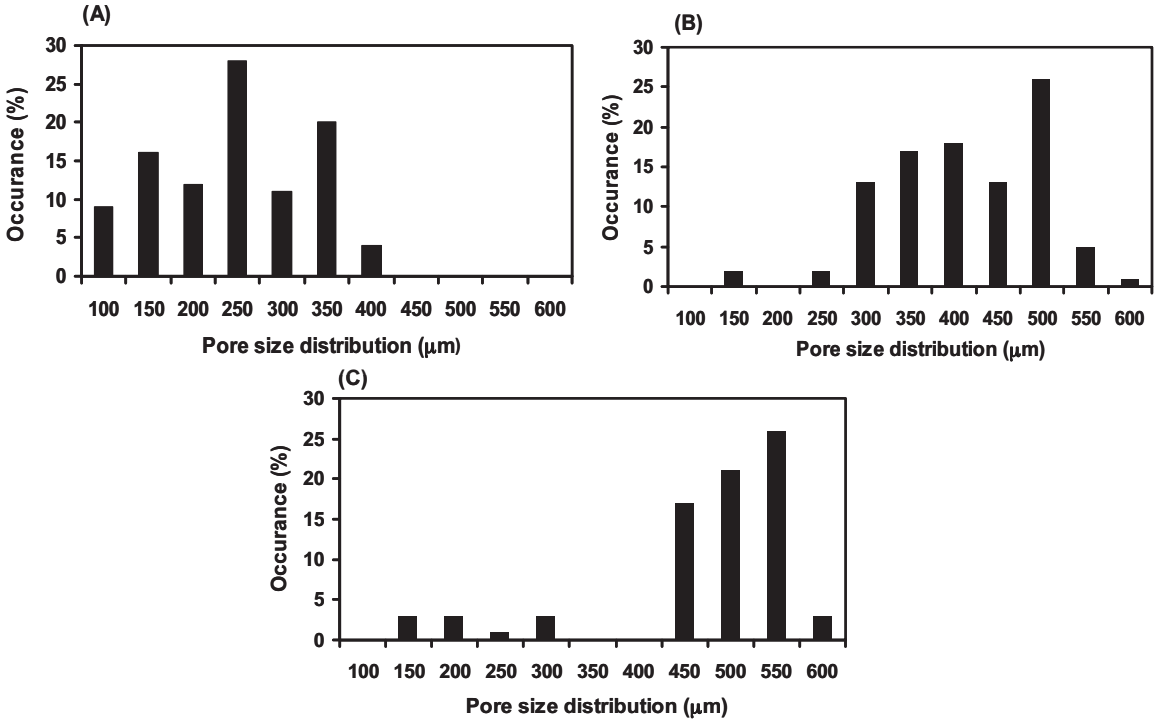

Fig. 4. Normalized pore size distribution of the PCL scaffolds fabricated using NaCl particles sizes of 100–300 μm (A), 300–500 μm (B), and 500–700 μm (C). (A salt concentration of 30 wt% was used.)

Table 1
Effect of gas foaming parameters on leaching ratio, average pore sizes and porosity of PCL scaffold produced by using gas foaming/salt leaching process.

P_s (bar)	T_s (°C)	S_t (h)	DPR (bar/min)	φ (%)	Average pore size (μm)	Porosity (%)
65	34	1	15	33	210 ± 20	23.1 ± 3.2
65	70	1	15	100	540 ± 18	91.1 ± 1.2
65	100	1	15	100	530 ± 21	89.2 ± 3.3
30	70	1	15	80	320 ± 15	51.9 ± 4.5
100	70	1	15	70	310 ± 15	64.2 ± 2.1
65	70	2	15	100	545 ± 10	91.2 ± 2.9
65	70	1	400	97	158 ± 10	60.1 ± 1.1

temperature of 34 °C was used to investigate the effects of processing parameters on the pore morphology of fabricated PCL scaffolds.

The effects of the gas foaming process variables including P_s, T_s, S_t, and DPR on the pore characteristics of PCL and φ were determined. T_s was varied between 34 °C and 100 °C and P_s in the range of 30–100 bar to investigate the effect of T_s and P_s. Two different rates of depressurization including 15 bar/min and 400 bar/min, and S_t of 1 h and 2 h were also used to investigate the effect of DPR and S_t on the pore size of PCL scaffolds, respectively.

3.3. Effect of saturation temperature (T_s)

The effect of T_s on the pore morphology of fabricated PCL scaffolds was assessed at 65 bar for 1 h and using DPR of 15 bar/min. As shown in Fig. 5 and Table 1, the average pore sizes of PCL scaffolds were significantly enhanced from 210 ± 20 μm to 540 ± 18 μm, when T_s was increased from 34 °C to 70 °C ($p < 0.01$). In addition, only 33% of salt particles leached out when T_s of 34 °C was used, confirming lower pore interconnectivity. In comparison, at T_s of 70 °C complete salt removal could be obtained (Table 1). These results were in agreement with decreasing the porosity of scaffolds fabricated at lower saturation temperature, 23.1 ± 3.2% compared to 91.1 ± 1.2%. An elevation of T_s from 70 °C to 100 °C had negligible effect on the pore sizes and porosity of fabricated scaffolds; this can be explained by the effect of CO_2 pressure on PCL melting point depression and also variation of the CO_2 density at these two temperatures.

Increasing T_s reduces the viscosity of PCL, which results in the diffusion of CO_2 within the polymer matrices and formation of scaf-

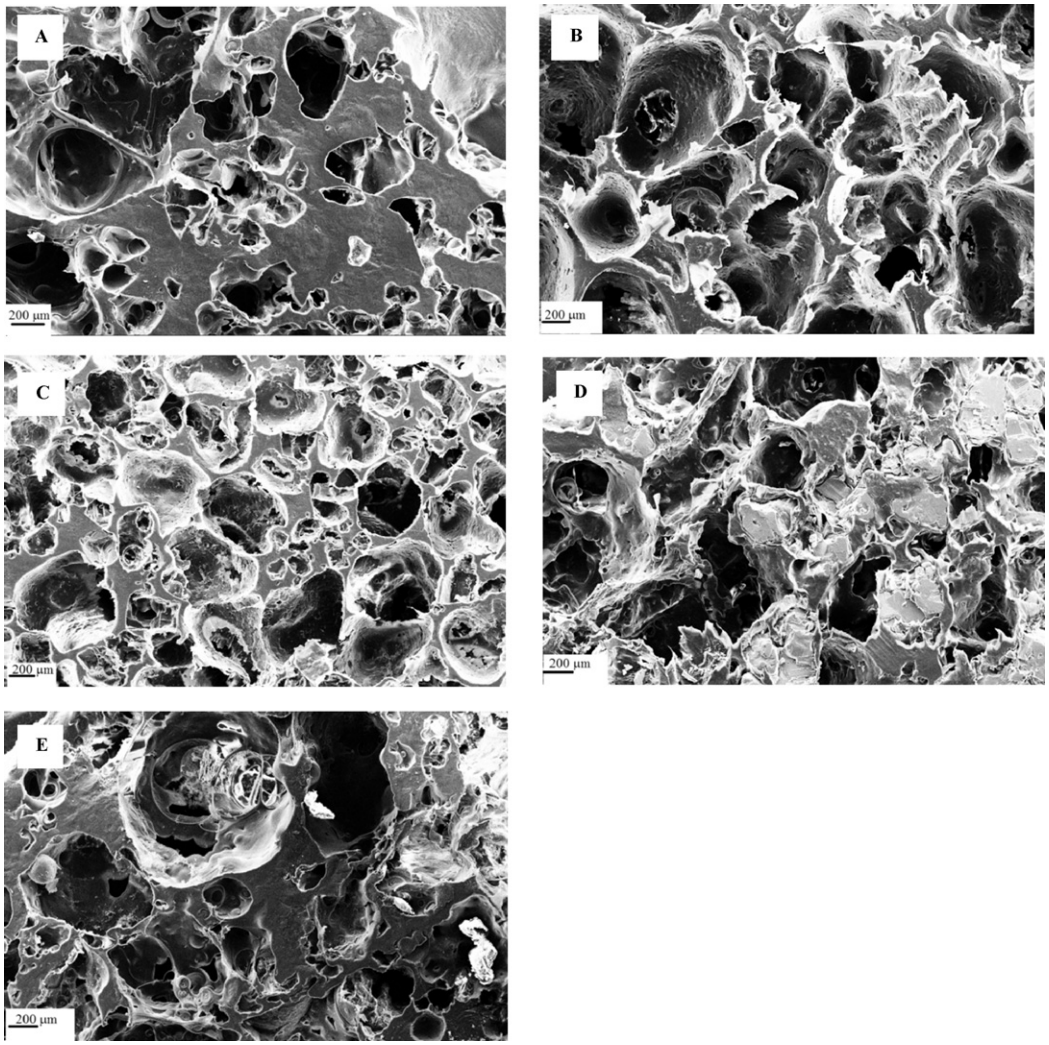

Fig. 5. SEM images of PCL scaffolds fabricated using the gas foaming/salt leaching process with a T_s of 34 °C and 65 bar (A), 70 °C and 65 bar, (B), 100 °C and 65 bar (C), 70 °C and 30 bar (D), and 70 °C and 100 bar (E) (DPR of 15 bar/min, and S_t of 1 h were used).

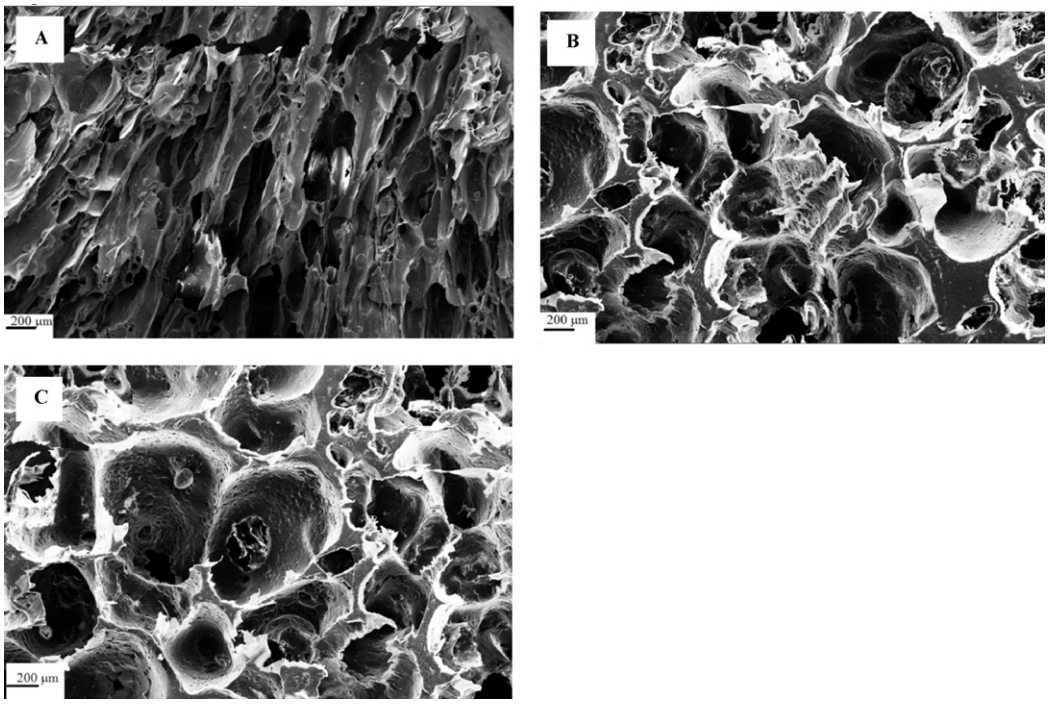

Fig. 6. SEM images of PCL scaffold fabricated by the gas foaming/salt leaching process using DPR of 400 bar/min and St of 1 h (A), DPR of 15 bar/min and St of 2 h (B), and DPR of 15 bar/min and St of 1 h, (P_s of 65 bar and T_s of 70 °C were used).

folds with larger pores [15,29]. The PCL melting point is decreased from 60 °C to 46 °C when the CO_2 pressure is increased from 1 bar to 65 bar [30]; therefore, in this study PCL was melted at T_s above 46 °C and pressures higher than 60 bar. NIST REFPROP software was used to determine CO_2 density at various operating conditions. The density of CO_2 slightly decreased from 150 kg/m^3 to 145 kg/m^3 at 65 bar, when the temperature was increased from 70 °C to 100 °C. Therefore, the amount of CO_2 dissolved in molten PCL did not significantly change by raising temperature. It can be concluded that T_s of 70 °C was adequate for PCL gas foaming/salt leaching process.

3.4. Effect of saturation pressure (P_s)

The P_s may have a significant impact on pore characteristics of PCL scaffolds. Previous studies demonstrated that no porosity is formed in PCL when it is pressurized with CO_2 at 70 °C and 30 bar [28]. However, increasing the processing pressure to 59 bar results in the formation of PCL scaffolds with average pore sizes of 250 μm [28]. In contrast, Tai et al. showed that the pore sizes of PLGA scaffolds fabricated by a gas foaming process are reduced when the processing pressure is increased from 60 bar to 150 bar [31]. In this study, gas foaming was conducted at T_s = 70 °C, DPR = 15 bar/min, and S_t = 1 h to investigate the effect of P_s on φ and pore sizes of PCL scaffold (Table 1). As shown in Fig. 5, increasing P_s from 30 bar to 65 bar significantly increased the pore sizes of PCL from 320 ± 15 μm to 540 ± 18 μm ($p < 0.01$). The effect of pressure on pore sizes can be explained by polymer plasticization and increasing CO_2 solubility in the molten phase at elevated pressures. A further increase of P_s to 100 bar reduced the average pore size of fabricated scaffolds to 310 ± 15 μm; increasing the amount of CO_2 in the polymer phase increased gas nucleation density during the depressurization stage, resulting in the production of a large number of smaller pores [15]. Furthermore, it has been reported that the melting temperature of PCL decreases from 46 °C to 26 °C, when CO_2 pressure is increases from 65 bar to 100 bar [30]. Therefore, at a foaming temperature of 34 °C and 65 bar, the PCL was not in a molten phase and solidified around the generated gas bubbles during depressurization; this resulted in the formation of large pores. However, at 34 °C and 100 bar; PCL was maintained in a molten phase during the depressurization stage which led to the generation of smaller pores.

As shown in Table 1, salt particles had completely leached out when using a P_s of 65 bar; however, φ was 80% and 70%, when the PCL was pressurized to 30 bar and 100 bar, respectively. Moreover, highest porosity, 91.1 ± 1.2% was achieved when a saturation pressure of 65 bar was selected, as shown in Table 1. Therefore, a P_s of 65 bar was selected to fabricate PCL scaffold.

3.5. Effect of depressurization rates (DPR)

The effect of DPR on pore morphology of PCL scaffolds was investigated by performing gas foaming at P_s = 65 bar, T_s = 70 °C, and S_t = 1 h. As shown in Fig. 6, fast depressurization (400 bar/min) resulted in the formation of non-homogenous PCL scaffolds with average pore sizes of 158.1 ± 10 μm. The pore sizes of fabricated PCL scaffolds were increased to 540 ± 18 μm, when the DPR was decreased to 15 bar/min (Table 1). Tai et al. also reported the formation of non-homogenous structure of PLA scaffold produced at 35 °C, 230 bar for 1 h using a relatively fast depressurization of 115 bar/min; however, decreasing the DPR to 2 bar/min resulted in the formation of uniform PLA scaffolds with larger pores [31]. Lowering DPR can provide extra time for the gas nuclei to grow and generate larger pores [15,31].

3.6. Effect of soaking time (S_t)

The effect of S_t on the pore morphology of fabricated PCL scaffolds was assessed at 65 bar, 70 °C for, and using DPR of 15 bar/min. As shown in Table 1 and Fig. 6, S_t had a negligible effect on the pore sizes and porosity of PCL scaffolds; increasing S_t from 1 h to

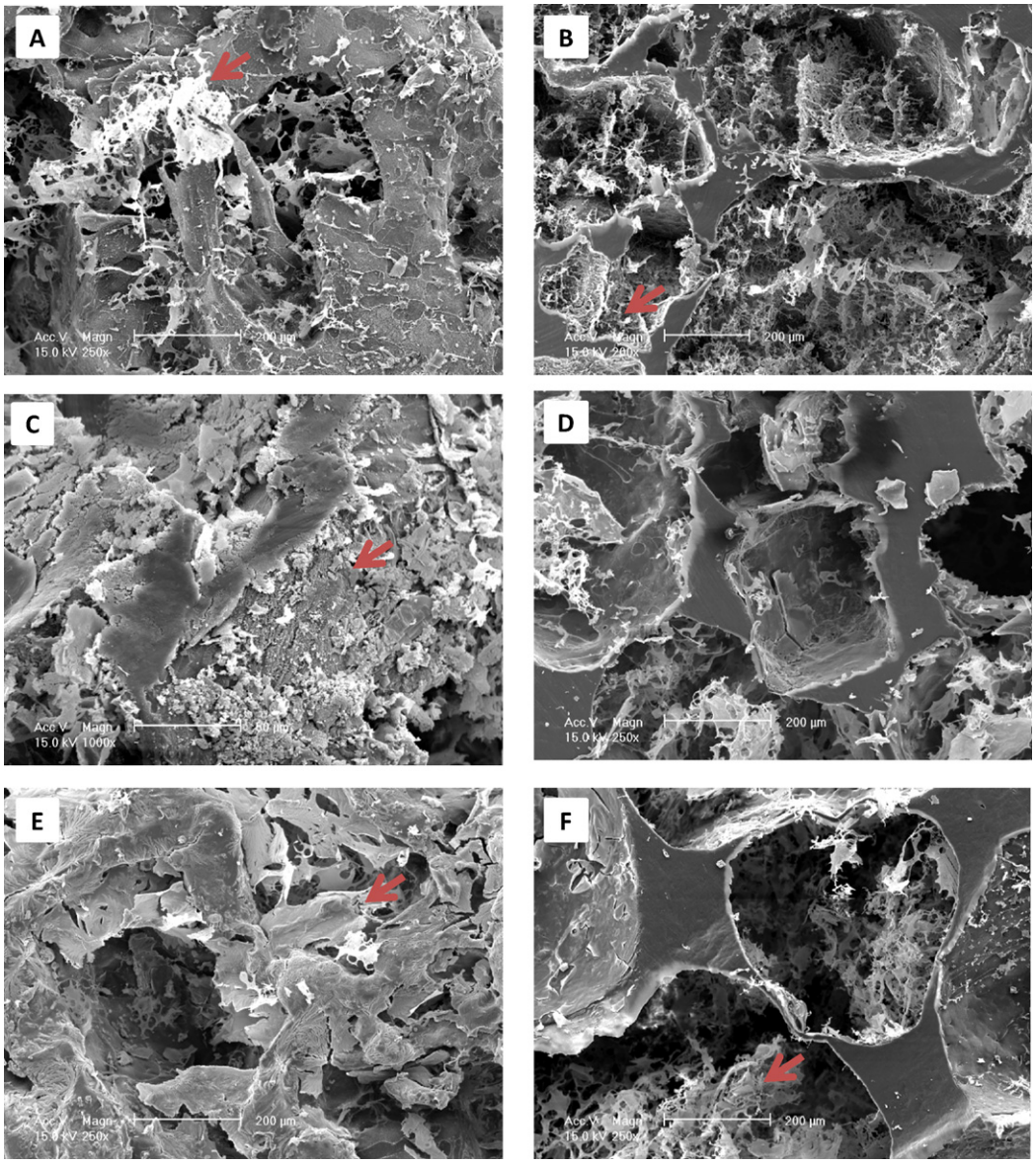

Fig. 7. SEM images of PCL/elastin composites fabricated using high pressure CO_2 (A and B), atmospheric pressure (C and D), and vacuum (E and F). Top surfaces are shown in A, C, and E; cross-sections in B, D, and F (arrows show the cross-linked elastin within the PCL scaffold).

2 h slightly changed the average pore size from 540 ± 18 μm to 545 ± 5 μm, and the porosity of both samples porosity was approximately 91%. This indicates that CO_2 saturated the PCL phase within 1 h because of the high mass transfer properties of CO_2 and also the small size of sample used in this study. Consequently, a soaking time of 1 h was considered adequate for the generation of appropriate pore sizes in the PCL scaffolds.

The porosity of a scaffold greatly affects the cellular adhesion and proliferation [13]. A highly porous scaffold was obtained for polymers such as PCL, PLA, and PLGA by using gas foaming/salt leaching process [23,31]. This process was efficient to create highly interconnected porous structures with porosity above 70% for these polymers [31]. It was also reported that 87% porosity was achieved for a PCL scaffold using 30 wt% salt concentration, and gas foaming by CO_2 at 65 bar and 70 °C [23]. The porosity of the PCL scaffold fabricated in this study was 91%. Interconnecting porosity achieved by gas foaming salt/leaching for PCL was further evidenced by cell infiltration into the construct acquired for this PCL/elastin scaffold in our recent study [26].

3.7. Fabrication of PCL/elastin composites

PCL/elastin composites were prepared under three different conditions: atmospheric pressure, vacuum, and high pressure CO_2. We have previously shown that an elastin hydrogel is formed within 24 h when cross-linked at 37 °C under atmospheric pressure. In contrast, the hydrogel can be fabricated in less than 1 h when the cross-linking reaction is performed under high pressure CO_2 [32]. Therefore, PCL scaffolds were soaked in elastin solution containing GA for 1 h at high pressure and 24 h under vacuum and atmospheric conditions to form composite constructs.

FTIR, SEM and gravimetric techniques were used to assess the efficiency of each process for the creation of homogenous 3D hybrid scaffolds. The presence of cross-linked elastin on the top surface (Fig. 7A) and within the cross section (Fig. 7B) of PCL scaffolds fabricated under high pressure CO_2 confirmed that elastin uniformly penetrated within the 3D structure of PCL under these conditions. The composite samples comprised two pore size components: 500 μm-sized PCL components and the smaller pores of

elastin hydrogels, similar to those produced previously [32]. In contrast, immersing the PCL scaffold in an elastin solution under atmospheric conditions resulted in the formation of a layer of crosslinked elastin on the top surface of the PCL foam with no penetration into the 3D structure (Fig. 7C and D). This effect might be due to the surface tension of the water phase that impeded solution penetration into the pores of PCL. Atmospheric conditions are therefore only useful for the formation of an elastin surface coating of PCL scaffolds. Impregnation of PCL scaffolds with elastin under vacuum conditions for 24 h slightly improved the penetration of elastin into the PCL scaffold, but the elastin was not homogenously distributed throughout the PCL structure as shown in Fig. 7E and F.

FTIR spectra of an elastin hydrogel showed two main peaks at 1535 cm^{-1}, and 1655 cm^{-1} corresponding to the amide II and amide I bands, respectively (Fig. 8). Similar peaks were observed for bovine elastin and *k*-elastin [33], human elastin [34], bovine tropoelastin [35], α-elastin [36,37], two elastin-like poly(pentapeptides) [38], and synthetic elastin hydrogel [39]. The FTIR spectra of PCL showed a main peak at 1725 cm^{-1} attributed to C=O stretching; this peak was also observed in previous studies for electrospun PCL samples [40]. The presence of peaks assigned to PCL and elastin on the top surface and 1 mm and 2 mm into the hybrid scaffold fabricated at high pressure CO_2 confirmed the presence of elastin in all layers of composites (Fig. 8A). However, FTIR analysis on hybrid scaffolds produced under vacuum demonstrated elastin penetration up to approximately 1 mm into the PCL scaffold as shown in Fig. 8B. The results of FTIR and SEM analysis confirmed that high pressure CO_2 was more efficient than the other techniques used in this study for the production of homogenous 3D hybrid PCL/elastin scaffolds.

The weight gain and water uptake of composites fabricated under high pressure CO_2 and vacuum are shown in Table 2. Samples fabricated under vacuum exhibited lower mass gain of 3 ± 0.08 wt% compared with those produced at high pressure CO_2 (15 ± 0.07 wt%). This was due to an increased introduction of elastin into the pores of PCL scaffolds when high pressure CO_2 was used for composite fabrication compared to vacuum.

Table 2
The weight gain and water uptake ratio of PCL/elastin composites fabricated by using high pressure CO_2 and vacuum.

Composite scaffolds	Weight gain (wt%)	Water uptake ratio (g liquid/g polymer)
High pressure CO_2	15 ± 0.07	3.5 ± 0.1
Vacuum	3 ± 0.08	1.1 ± 0.1

The presence of elastin within the 3D PCL matrices imparted hydrophilicity to the composite scaffolds and affected their water uptake properties. As shown in Table 2, hybrid scaffolds fabricated under high pressure CO_2 exhibited higher water uptake ratio of 3.5 ± 0.1 g liquid/g polymer compared with the one produced under vacuum conditions (1.1 ± 0.1 g liquid/g polymer). Generally, the water uptake ratios of composites fabricated under either high pressure CO_2 or vacuum were higher than PCL scaffolds (0.03 ± 0.005 g liquid/g polymer).

The compressive modulus of fabricated hybrid scaffolds was higher than of pure elastin hydrogel and lower than of PCL scaffold [26]. The compressive modulus of PCL/elastin composites was 1.30 ± 0.07 MPa, which slightly exceeded the target value for cartilage repair, 0.5–1 MPa [26].

The stability of adsorbed crosslinked elastin within the 3D structure of composites was evaluated by calculating the elastin retention ratio after soaking in PBS for 1, 2, and 7 days. As confirmed by FITR and weight gain analyses, elastin diffusion throughout the 3D PCL scaffolds was higher for the PCL/elastin composites fabricated under high pressure CO_2 compared to those produced by using vacuum. Therefore, elastin stability was only determined for the composites fabricated under high pressure CO_2. As shown in Fig. 9, elastin retention ratio diminished from 86.4 ± 2(w/w) % at day 1 to 72.1 ± 1(w/w) % and 70.7 ± 2(w/w) % at days 2 and 7 of

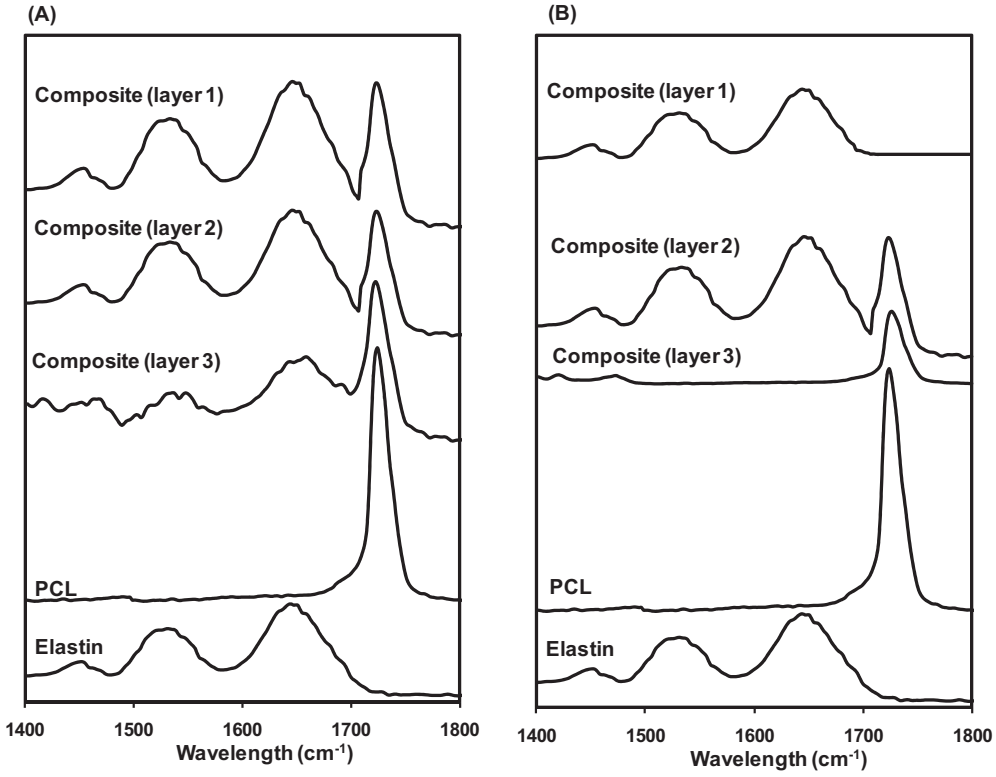

Fig. 8. Fourier transform infrared (FTIR) spectra for pure α-elastin hydrogel, PCL, and composite PCL/α-elastin scaffolds produced under high pressure CO_2 (A), and vacuum (B) (Layer 1: top surface, Layer 2: 1 mm depth, Layer 3: 2 mm depth).

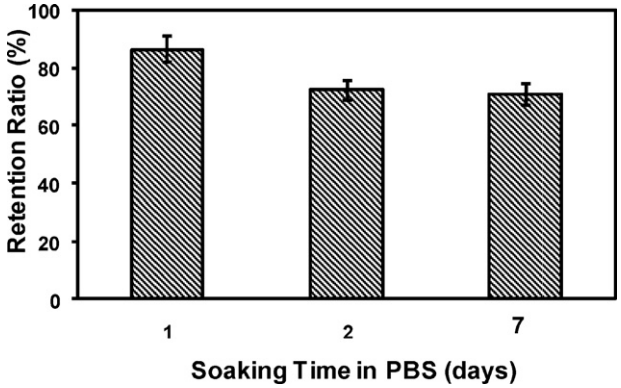

Fig. 9. Elastin retention in composite PCL/elastin scaffolds fabricated under high pressure CO_2 on days 1, 2, and 7 of immersion in PBS.

soaking, respectively. The decrease in retention ratio on day 2 of immersing in PBS may be due to the removal of excess uncross-linked elastin from the composites during washing step. However, there was no significant change in retention ratio of elastin after the second day of soaking. This confirmed the stability of cross-linked elastin within the pores of hybrid scaffolds fabricated under high pressure CO_2.

The hybrid scaffold was comprised of large size pores of PCL construct (average size of 540 μm) and small size pores of elastin hydrogel (average size of 50 μm). The results of *in vitro* studies confirmed the proliferation of chondrocytes into the 3D structure of hybrid scaffold processed by dense gas CO_2 [26]. These results demonstrate that the pores in the composite construct were interconnected and nutrient and oxygen could penetrate through the 3D structure of composite scaffold.

Hybrid natural/synthetic scaffolds such as chitosan/PCL [41], collagen/PCL [6], chitosan/PLLA [42], and alginate/2-hydroxyethylmethacrylate (HEMA) [43] have been constructed for tissue engineering applications; generally, a porous structure of one polymer is immersed in a solution of the other polymer under vacuum to form these composites [6,41,42]. Mei et al. made PCL/chitosan scaffolds by soaking prefabricated PCL foams, using solvent casting/particle leaching, in a solution of chitosan under vacuum pressure. The weight gain of PCL/chitosan composite is 8.4 ± 0.1 wt% when 20 mg/ml of chitosan solution is used [41]. Porous alginate/HEMA hybrids can be made by supercritical CO_2 assisted impregnation of alginate foams with HEMA and a cross-linking agent [43] where the pore size and weight gains of fabricated composites are in the range of 21–105 μm and 40–170 wt%, respectively, depending on the HEMA and crosslinker concentrations. Jiao et al. produced a hybrid chitosan/PLLA scaffold by immersing PLLA scaffold, produced by a solvent casting/salt leaching process, into a 1.5 wt% chitosan solution using vaccum [43]. When the chitosan concentration is higher than 1.5 wt%, it is difficult for the solution to penetrate into the PLLA sponge due to its high viscosity [43]. In our study, the negligible diffusion of cross-linked elastin within 3D PCL scaffold fabricated under vacuum appears to be due to the high viscosity of the cross-linking elastin solution within 24 h of cross-linking time. However, elastin solution penetrated into 3D structure of porous PCL under high pressure and cross-linked. High pressure CO_2 was the driving force to overcome the surface tension and viscosity of elastin solution that can impede diffusion of solution into the porous structure. High pressure CO_2 allowed us to overcome limitations posed by more conventional methods (e.g. vacuum) such as long processing time (e.g. 24 h) [6,8], use of organic solvent [6,8,41], and the formation of 2D structure [6].

4. Conclusions

Dense gas processes were successfully used to create both porous PCL scaffolds with a high degree of interconnectivity and homogenous 3D PCL/elastin hybrid scaffolds. Porous PCL scaffolds with average pore sizes larger than 500 μm and porosity of 91% were produced using a gas foaming/salt leaching process. The fabrication of hybrid scaffolds at atmospheric pressure was efficient for surface modification of PCL. Conducting the process under vacuum allowed for elastin penetration up to 1 mm into the samples which may be useful for the fabrication of thin hybrid scaffolds. However, the fabrication of PCL/elastin composites under high pressure CO_2 enabled elastin penetration throughout the 3D PCL scaffolds. The water uptake ratio of hybrid scaffolds fabricated using high pressure CO_2 was 3-fold higher than those produced under vacuum. Composites fabricated using high pressure CO_2 may be very useful for tissue engineering applications.

Acknowledgments

The authors acknowledge financial support from the Australian Research Council and the National Health and Medical Research Council.

References

[1] D.V. Bax, D.R. McKenzie, A.S. Weiss, M.M.M. Bilek, The linker-free covalent attachment of collagen to plasma immersion ion implantation treated polytetrafluoroethylene and subsequent cell-binding activity, Biomaterials 31 (9) (2009) 2526–2534.
[2] N. Annabi, J.W. Nichol, X. Zhong, C. Ji, S. Koshy, A. Khademhosseini, F. Dehghani, Controlling the porosity and microarchitecture of hydrogels for tissue engineering, Tissue Engineering: Part B 16 (4) (2010) 371–380.
[3] P.B. Malafaya, G.A. Silva, R.L. Reis, Natural-origin polymers as carriers and scaffolds for biomolecules and cell delivery in tissue engineering applications, Advanced Drug Delivery Reviews 59 (4–5) (2007) 207–233.
[4] A. Sarasam, S.V. Madihally, Characterization of chitosan–polycaprolactone blends for tissue engineering applications, Biomaterials 26 (2005) 5500–5508.
[5] L. Averousa, L. Moro, P. Dole, C. Fringantc, Properties of thermoplastic blends: starch–polycaprolactone, Polymer 41 (2000) 4157–4167.
[6] A.G.A. Coombes, E. Verderio, B. Shaw, X. Li, M. Griffin, S. Downes, Biocomposites of non-crosslinked natural and synthetic polymers, Biomaterials 23 (2002) 2113–2118.
[7] D. Pankajakshan, K.V. Kalliyana, L.K. Krishnan, Vascular tissue generation in response to signaling molecules integrated with a novel poly(Îμ-caprolactone)–fibrin hybrid scaffold, J. Tissue Engineering and Regenerative Medicine 1 (5) (2007) 389–397.
[8] G. Chen, T. Ushida, T. Tateishi, A biodegradable hybrid sponge nested with collagen microsponges, J. Biomedical Materials Research 51 (2) (2000) 273–279.
[9] E. Sachlos, J.T. Czernuszka, Making tissue engineering scaffolds work, European Cells & Materials 5 (2003) 29.
[10] J. Stitzel, J. Liu, S.J. Lee, M. Komura, J. Berry, S. Soker, G. Lim, M. Van Dyke, R. Czerw, J.J. Yoo, A. Atala, Controlled fabrication of a biological vascular substitute, Biomaterials 27 (7) (2006) 1088–1094.
[11] M.K.C. Ng, A.S. Weiss, S.G. Wise, Tropoelastin-based protoelastin biomaterials of high flexibility for use in vascular prosthetic applications. WO 2008/037028.
[12] S. Heydarkhan-Hagvall, K. Schenke-Layland, A.P. Dhanasopon, F. Rofail, H. Smith, B.M. Wu, R. Shemin, R.E. Beygui, W.R. MacLellan, Three-dimensional electrospun ECM-based hybrid scaffolds for cardiovascular tissue engineering, Biomaterials 29 (19) (2008) 2907–2914.
[13] S.-M. Lien, L.-Y. Ko, T.-J. Huang, Effect of pore size on ECM secretion and cell growth in gelatin scaffold for articular cartilage tissue engineering, Acta Biomaterialia 5 (2) (2009) 670–679.
[14] Z.-M. Xu, X.-L. Jiang, T. Liu, G.-H. Hu, L. Zhao, Z.-N. Zhu, W.-K. Yuan, Foaming of polypropylene with supercritical carbon dioxide, J. Supercritical Fluids 41 (2) (2007) 299–310.
[15] H. Tai, V.K. Popov, K.M. Shakesheff, S.M. Howdle, Putting the fizz into chemistry: applications of supercritical carbon dioxide in tissue engineering, drug delivery and synthesis of novel block copolymers, Biochemical Society Transactions 35 (3) (2007) 516–521.
[16] J.J.A. Barry, M.M.C.G. Silva, V.K. Popov, K.M. Shakesheff, S.M. Howdle, Supercritical carbon dioxide: putting the fizz into biomaterials, Philosophical Transactions Series A: Mathematical, Physical and Engineering Sciences 364 (1838) (2006) 249–261.
[17] J.J.A. Barry, M.M.C.G. Silva, S.H. Cartmell, R.E. Guldberg, C.A. Scotchford, S.M. Howdle, Porous methacrylate tissue engineering scaffolds: using carbon dioxide to control porosity and interconnectivity, J. Materials Science 41 (13) (2006) 4197–4204.

[18] C.B. Park, D.F. Baldwin, N.P. Suh, Effect of the pressure drop rate on cell nucleation in continuous processing of microcellular polymers, Polymer Engineering and Science 35 (5) (1995) 432–440.
[19] D.J. Mooney, D.F. Baldwin, N.P. Suh, J.P. Vacanti, R. Langer, Novel approach to fabricate porous sponges of poly(D,L-lactic-co-glycolic acid) without the use of organic solvents, Biomaterials 17 (14) (1996) 1417–1422.
[20] S.K. Goel, E.J. Beckman, Generation of microcellular polymeric foams using supercritical carbon dioxide. II. Cell growth and skin formation, Polymer Engineering and Science 34 (14) (1994) 1148–1156.
[21] D. Hutmacher, Scaffolds in tissue engineering bone and cartilage, Biomaterials 21 (2000) 2529–2543.
[22] L.D. Harris, B.S. Kim, D.J. Mooney, Open pore biodegradable matrices formed with gas foaming, J. Biomedical Materials Research 42 (3) (1998) 396–402.
[23] A. Salerno, S. Iannace, P.A. Netti, Open-pore biodegradable foams prepared via gas foaming and microparticulate templating, Macromolecular Biosciences 8 (2008) 655–664.
[24] N. Annabi, S.M. Mithieux, A.S. Weiss, F. Dehghani, Cross-linked open-pore elastic hydrogels based on tropoelastin, elastin and high pressure CO_2, Biomaterials 31 (7) (2010) 1655–1665.
[25] S.M. Mithieux, A.S. Weiss, Elastin, Advances in Protein Chemistry 70 (2005) 437–461.
[26] N. Annabi, A. Fathi, S.M. Mithieux, P. Martens, A.S. Weiss, F. Dehghani, The effect of elastin on chondrocyte adhesion and proliferation on poly (ε-caprolactone) elastin composites, Biomaterials 32 (2011) 1517–1525.
[27] S. Blacher, C. Calberg, G. Kerckhofs, A. Léonard, M. Wevers, R. Jérôme, J.-P. Pirard, The porous structure of biodegradable scaffolds obtained with supercritical CO_2 as foaming agent, Studies in Surface Science and Catalysis 160 (2007) 681–688.
[28] E. Di Maio, G. Mensitieri, S. Iannace, L. Nicolais, W. Li, R.W. Flumerfelt, Structure optimization of polycaprolactone foams by using mixtures of CO_2 and N_2 as blowing agents, Polymer Engineering and Science 45 (3) (2005) 432–441.
[29] K.A. Arora, A.J. Lesser, T.J. McCarthy, Preparation and characterization of microcellular polystyrene foams processed in supercritical carbon dioxide, Macromolecules 31 (14) (1998) 4614–4620.
[30] Z. Lian, S. Epstein, C. Blenk, A. Shine, Carbon dioxide-induced melting point depression of biodegradable semicrystalline polymers, J. Supercritical Fluids 39 (2006) 107–117.
[31] H. Tai, M.L. Mather, D. Howard, W. Wang, L.J. White, J.A. Crowe, S.P. Morgan, A. Chandra, D.J. Williams, S.M. Howdle, K.M. Shakesheff, Control of pore size and structure of tissue engineering scaffolds produced by supercritical fluid processing, European Cells & Materials 14 (2007) 64–77.
[32] N. Annabi, S.M. Mithieux, A.S. Weiss, F. Dehghani, The fabrication of elastin-based hydrogels using high pressure CO_2, Biomaterials 30 (1) (2009) 1–7.
[33] L. Debelle, A.J.P. Alix, M.-P. Jacob, J.-P. Huvenne, M. Berjot, B. Sombret, P. Legrand, Bovine elastin and *k*-elastin secondary structure determination by optical spectroscopies, J. Biological Chemistry 270 (44) (1995) 26099–26103.
[34] L. Debelle, A.J.P. Alix, S.M. Wei, M.-P. Jacob, J.-P. Huvenne, M. Berjot, P. Legrand, The secondary structure and architecture of human elastin, European Journal of Biochemistry 258 (2) (1998) 533–539.
[35] L. Debelle, A.J.P. Alix, Optical spectroscopic determination of bovine tropoelastin molecular model, J. Molecular Structure 348 (1995) 321–324.
[36] M. Mammi, L. Gotte, G. Pezzin, Evidence for order in the structure of alpha-elastin, Nature 220 (5165) (1968) 371–373.
[37] F. Dehghani, N. Annabi, P. Valtchev, S.M. Mithieux, A.S. Weiss, S.G. Kazarian, F.H. Tay, Effect of dense gas CO_2 on the coacervation of elastin, Biomacromolecules 9 (4) (2008) 1100–1105.
[38] P. Schmidt, J. Dybal, J.C. Rodriguez-Cabello, V. Reboto, Role of water in structural changes of poly(AVGVP) and poly(GVGVP) studied by FTIR and Raman spectroscopy and ab initio calculations, Biomacromolecules 6 (2) (2005) 697–706.
[39] S.M. Mithieux, J.E.J. Rasko, A.S. Weiss, Synthetic elastin hydrogels derived from massive elastic assemblies of self-organized human protein monomers, Biomaterials 25 (20) (2004) 4921–4927.
[40] R. Nirmala, K.T. Nam, D.K. Park, B. Woo-il, R. Navamathavan, H.Y. Kim, Structural, thermal, mechanical and bioactivity evaluation of silver-loaded bovine bone hydroxyapatite grafted poly([epsilon]-caprolactone) nanofibers via electrospinning, Surface and Coating Technology 205 (1) (2010) 174–181.
[41] N. Mei, G. Chen, P. Zhou, X. Chen, Z.-Z. Shao, L.-F. Pan, C.-G. Wu, Biocompatibility of poly(e-caprolactone) scaffold modified by chitosan-the fibroblasts proliferation in vitro, J. Biomaterials Applications 19 (4) (2005) 323–339.
[42] Y. Jiao, Z. Liu, C. Zhou, Fabrication and characterization of PLLA–chitosan hybrid scaffolds with improved cell compatibility, J. Biomedical Materials Research, Part A 80A (4) (2007) 820–825.
[43] S. Partap, A.K. Hebb, I. ur Rehman, J.A. Darr, Formation of porous natural-synthetic polymer composites using emulsion templating and supercritical fluid assisted impregnation, Polymer Bulletin 58 (5-6) (2007) 849–860.